

Endovenous Administration of Bone Marrow-Derived Multipotent Mesenchymal Stromal Cells Prevents Renal Failure in Diabetic Mice

Fernando Ezquer,¹ Marcelo Ezquer,^{1,2} Valeska Simon,¹ Fabian Pardo,³ Alejandro Yañez,³ Daniel Carpio,⁴ Paulette Conget¹

Twenty-five to 40% of diabetic patients develop diabetic nephropathy, a clinical syndrome that comprises renal failure and increased risk of cardiovascular disease. It represents the major cause of chronic kidney disease and is associated with premature morbimortality of diabetic patients. Multipotent mesenchymal stromal cells (MSC) contribute to the regeneration of several organs, including acutely injured kidney. We sought to evaluate if MSC protect kidney function and structure when endovenously administered to mice with severe diabetes. A month after nonimmunologic diabetes induction by streptozotocin injection, C57BL/6 mice presented hyperglycemia, glycosuria, hypoinsulinemia, massive β -pancreatic islet destruction, low albuminuria, but not renal histopathologic changes (DM mice). At this stage, one group of animals received the vehicle (untreated) and other group received 2 doses of 0.5×10^6 MSC/each (MSC-treated). Untreated DM mice gradually increased urinary albumin excretion and 4 months after diabetes onset, they reached values 15 times higher than normal animals. In contrast, MSC-treated DM mice maintained basal levels of albuminuria. Untreated DM mice had marked glomerular and tubular histopathologic changes (sclerosis, mesangial expansion, tubular dilatation, proteins cylinders, podocytes lost). However, MSC-treated mice showed only slight tubular dilatation. Observed renoprotection was not associated with an improvement in endocrine pancreas function in this animal model, because MSC-treated DM mice remained hyperglycemic and hypoinsulinemic, and maintained few remnant β -pancreatic islets throughout the study period. To study MSC biodistribution, cells were isolated from isogenic mice that constitutively express GFP (MSC^{GFP}) and endovenously administered to DM mice. Although at very low levels, donor cells were found in kidney of DM mice 3 month after transplantation. Presented preclinical results support MSC administration as a cell therapy strategy to prevent chronic renal diseases secondary to diabetes.

Biol Blood Marrow Transplant 15: 1354-1365 (2009) © 2009 American Society for Blood and Marrow Transplantation

KEY WORDS: Multipotent mesenchymal stromal cells, Mesenchymal stem cells, Renal failure, Diabetes, Renoprotection

INTRODUCTION

Diabetes mellitus (DM) is one of the current main threats to public health [1]. According to the World Health Organization, the total number of people

with diabetes is projected to rise from 171 million in the year 2000 to 366 million in 2030 [2]. About 25% to 40% of diabetic patients, within 20 to 25 years of the onset of type 1 or type 2 DM, will develop diabetic nephropathy (DN). A clinical syndrome that comprises renal failure and increased risk of cardiovascular disease [3]. DN represents the major cause of chronic kidney disease [4]. Thus, it is one of the most detrimental long-term complications of DM, and is highly associated with premature morbidity and mortality of diabetic patients [5].

In susceptible patients, DN follows a well-known temporal and clinical course. Microalbuminuria (low level of albumin excretion in urine) is the earliest detectable sign of kidney damage. It is associated with histologic changes, which include glomerular mesangial expansion, extracellular matrix deposition, and glomerular basement membrane thickening [6]. Macroalbuminuria appears later on, followed by

From the ¹Instituto de Ciencias, Facultad de Medicina Clínica Alemana Universidad del Desarrollo, Santiago, Chile; ²Instituto de Biología y Medicina Experimental de Cuyo, IMBECU-CONYCET, Mendoza, Argentina; ³Instituto de Bioquímica, Universidad Austral de Chile, Valdivia, Chile; and ⁴Instituto de Histología y Patología, Universidad Austral de Chile, Valdivia, Chile.

Financial disclosure: See Acknowledgments on page 1364.

Correspondence and reprint requests: Paulette A. Conget, PhD, Av. Las Condes 12438, Lo Barnechea, Santiago, Chile 7710162 (e-mail: pconget@udd.cl).

Received April 1, 2009; accepted July 24, 2009

© 2009 American Society for Blood and Marrow Transplantation

1083-8791/09/1511-0002\$36.00/0

doi:10.1016/j.bbmt.2009.07.022

a progressive decline in the glomerular filtration rate and marked histopathologic features. These include arteriolar hyalinosis, glomerulosclerosis, and tubulointerstitial fibrosis [7,8]. At this stage, even if patients were on dialysis, 21% of them will die within a year [9].

In DN, the interaction of metabolic and hemodynamic factors results in renal damage [8]. High mitochondrial oxidative stress, generated by the augmented glucose metabolism, leads to a reduction in the number of glomerular podocytes [10-12]. Kidney-activated macrophages maintain chronic inflammation and produce interleukin (IL)-1, tumor necrosis factor (TNF)- α , nitric oxide (NO), and reactive oxygen species, resulting in increased vascular permeability and renal cell death [13-15]. They also induce renal fibrosis because of the secretion of fibroblast growth factor (FGF) and transforming growth factor (TGF)- β [15,16]. Thus, in DN, all the ultrafiltration components (podocytes, fenestrated endothelial cells, and glomerular basement membrane) are affected.

To date, there is no cure to DN. Patients' management comprises the use of drugs to control hyperglycemia and blood pressure. If required, hemodialysis is prescribed [17,18]. Unfortunately, those treatments are very expensive, lifelong, and only helps to slow DN progression [19].

Multipotent mesenchymal stromal cells (also referred as mesenchymal stem cells [MSC]) are a population of self-renewable and undifferentiated cells present in the bone marrow (BM) and mesenchymal tissues of adult individuals [20]. It has been proved that MSC contribute to renal regeneration in animal models of kidney injury. In drug-induced acute renal failure, transplanted MSC engraft into the tubular epithelium and promote the restoration of necrotic segments [21,22]. MSC have also been successfully used in the experimental treatment of severe kidney diseases including glomerulonephropathy [23], and Alport syndrome [24]. Together, we have demonstrated that systemic administration of MSC into immunologically induced type 1 diabetic mice reduced microalbuminuria and preserved normal renal histology. By contrast, untreated type 1 diabetic mice were microalbuminuric and presented glomerular hyalinosis and mesangial expansion [25]. Observed renoprotection was associated with the concomitant improvement of diabetes condition because of the regeneration of insulin-producing cells and restriction of glucagon-producing cells. On the other hand, in an incomplete model of type 2 DM settled in immunodeficient nonobese diabetic (NOD)/severe combined immunodeficiency (SCID) mice, an intracardiac infusion of a large number of human MSC ($\sim 250 \times 10^6$ /kg body weight) resulted in the homing of donor cells into the kidneys. Unfortunately, it is not known whether this had any functional consequence, as animals did not present renal failure before the

intervention or during the follow-up period [26]. Thus, data already published suggest that MSC administration might be renoprotective in diabetic individuals. However, animal models previously used to test this only developed the earlier harbingers of DN (mild microalbuminuria and tubular and glomerular hyalinosis) [12,26]. Furthermore, it remains unknown if renoprotection is secondary or not to the improvement in endocrine pancreas function.

In the present work, we evaluated whether MSC are renoprotective when endovenously administered to nonimmunologically induced severe diabetic mice that, despite not sharing the etiology of either type 1 or type 2 DM, show a rapid progression of renal failure and develop most of its pathognomonic signs [27-30]. For this, 30 days after the massive cytotoxic destruction of insulin-producing cells by the injection of a single high dose of streptozotocin (STZ), C57BL/6 mice were separated in 2 groups: one group received the vehicle (untreated) and the other, 2 doses of 0.5×10^6 MSC/each (MSC treated). Before the intervention, and up to 90 days after it, kidney and pancreas function and structure were assessed (Figure 1). Data obtained for MSC-treated DM mice were compared against diabetic untreated and normal nondiabetic mice. Together, MSC biodistribution in severe nonimmunologically induced diabetic mice was evaluated 7 and 90 days after systemic administration of MSC isolated from isogenic mice that constitutively express GFP (MSC^{GFP}).

MATERIALS AND METHODS

Animals

C57BL/6 and C57BL/6-Tg(ACTB-EGFP)10sb/J mice (Jackson Laboratory, Bar Harbor, ME) were housed at constant temperature and humidity, with a 12:12 h light-dark cycle and unrestricted access to a standard diet and water. When required, animals were lightly anesthetized with sevoflurane (Abbott, Japan). All animal protocols used were approved by the Ethic Committee of Facultad de Medicina, Clinica Alemana-Universidad del Desarrollo.

Diabetes Induction

Eight-week-old male C57BL/6 mice were lightly anesthetized and received intraperitoneally 200 mg/kg STZ (Calbiochem, La Jolla, CA) immediately after dissolving in 0.1 M citrate buffer at pH 4.5 (DM mice) or citrate buffer only (normal mice). This protocol of STZ administration causes a massive cytotoxic nonimmunologic destruction of insulin-producing cells generating a severe hyperglycemia condition, which accelerates the appearance of the secondary complications associated to diabetes [31,32].

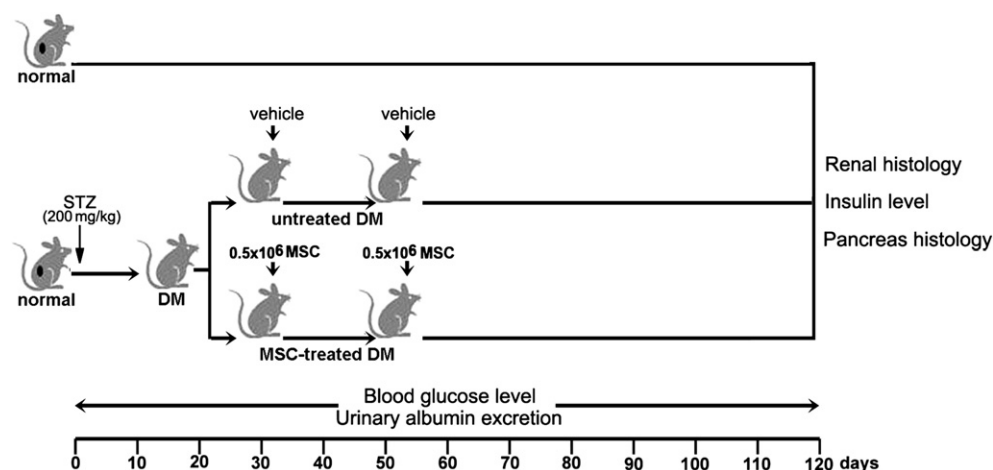


Figure 1. Protocol. To induce severe nonimmunologic diabetes, C57BL/6 adult male mice were injected with 200 mg/kg STZ (DM). Thirty and 51 days after, animals received via the tail vein the vehicle (untreated) or 0.5×10^6 MSC (MSC treated). During the follow-up period, urinary albumin excretion was determined every 20 days and blood glucose level every 3 days, to monitor kidney and pancreas function, respectively. At day 120 postdiabetes induction, kidney and pancreas structure were evaluated. Protocol was performed 3 times, and the total number of animals was 12 normal nondiabetic, 20 DM that received vehicle, and 20 DM that received MSC.

MSC isolation, ex vivo Expansion, and Characterization

Eight- to 10 week-old male C57BL/6 or C57BL/6-Tg(ACTB-EGFP)10sb/J mice were sacrificed by cervical dislocation. BM cells were obtained by flushing femurs and tibiae with sterile phosphate-buffered saline (PBS). After centrifugation, cells were resuspended in α -minimum essential medium (MEM) (Gibco, Auckland, NZ) supplemented with 10% selected fetal bovine serum (Gibco, Auckland, NZ) and 80 mg/mL gentamicin (Sanderson Laboratory, Chile) and plated at a density of 1×10^6 nucleated cells/cm². Nonadherent cells were removed after 72 hours by media change. When foci reach confluence, adherent cells were detached with 0.25% trypsin, 2.65 mM EDTA, centrifuged, and subcultured at 7000 cells/cm². After 2 subcultures, adherent cells were characterized according to their adipogenic and osteogenic differentiation potential, as previously described [33]. Although there is currently no consensus markers for murine MSC as there is for human MSC [34], immunophenotyping was performed by flow cytometry analysis after immunostaining with monoclonal antibodies (mAbs) against putative murine MSC markers: SCA-1 (APC-conjugated, eBioscience, San Diego, CA) and CD90 (FITC-conjugated, eBioscience) and hemopoietic lineage markers: B220, CD4, CD8 (PE-Cy5-conjugated, BD Biosciences Pharmingen, San Jose, CA) [35].

MSC Administration

Thirty and 51 days postdiabetes induction 0.5×10^6 MSC (or 0.5×10^6 MSC^{GFP}) were resuspended in 0.2 mL of 5% mice plasma and administered via the tail vein to lightly anesthetized mice (MSC-treated DM

mice). Untreated DM mice received 0.2 mL of 5% mice plasma.

Blood Glucose Determination

From nonfasted alert animals, blood samples were collected from the tail vein and glucose levels were determined with the glucometer system Accu-Chek Go from Roche Diagnostic (Mannheim, Germany).

Urinary Glucose Determination

Mice were kept in metabolic cages until they spontaneously urinated. Glucose levels were measured with the glucometer system Accu-Chek Go. To fit samples to the linear range of the glucometer system, urine was diluted in 0.9% NaCl.

Plasma Insulin Determination

Plasma insulin was assayed on blood obtained from the tail vein of fasted alert animals using a mouse-specific ELISA kit (Ultrasensitive Mouse Insulin ELISA; Mercodia, Uppsala, Sweden).

Urinary Albumin Determination

Excretion of urinary albumin was determined using albumin to creatinine ratio on morning spot urine collections. Mice were kept in metabolic cages until they spontaneously urinated. Urine albumin concentration was determined using a human immunoturbidimetric commercial kit from Orion Diagnostica (Espoo, Finland). Previously, we proved that the antibodies included in this kit crossreact with mouse albumin [25], as human and mouse albumins are 80% identical [36]. Urine creatinine concentration was determined by the kinetic modified Jaffe method using a kit from Applied Clinical Chemistry (Amposta, Spain) [25].

Kidney and Pancreas Histology

Mice were anesthetized by intramuscular injection of xylazine and ketamine and sacrificed by intracardiac injection of thiopental. Kidneys and pancreas were rapidly removed, fixed with 4% paraformaldehyde, and embedded in paraffin. Renal sections (4 μ m) were stained with PAS reagent and 4- μ m pancreatic sections were stained with hematoxylin-eosin. Slices were analyzed under light microscopy, focusing on kidney glomeruli and tubules and pancreas islets, respectively. Images were captured with a digital camera. Renal biopsies were analyzed at the same time, blinded, by the same specialized nephropathologist. Extend of glomerular damage was expressed as the percentage of glomeruli presenting glomerulosclerosis or mesangial expansion [37]. Tubular damage was graded, from 0 to 4, according to the presence or not of dilatation, proteins cylinders, and atrophy (0=no changes, 1=changes affecting <25% of the sample, 2=changes

affecting 25% to 50% of the sample, 3=changes affecting 50% to 75% of the sample, and 4=changes affecting 75% to 100% of the sample) [37].

Kidney Electron Microscopy Analysis

Kidneys were rapidly dissected out, and small pieces of renal cortex were fixed in 0.1 M phosphate-buffered 1.2% glutaraldehyde, postfixed in 1% osmium tetroxide and embedded in Epon resin. Ultra-thin sections were cut, double stained with uranyl acetate and lead citrate, and examined with a Phillips Morgagni electron microscope. Thickening of glomerular basement membrane was determined as described [38]. Briefly, glomerular capillary loops were photographed by electron microscopy and printed to an original magnification of 30,000 \times . Regions of the basement membrane were selected at random in glomeruli and the thickness of each region was measured.

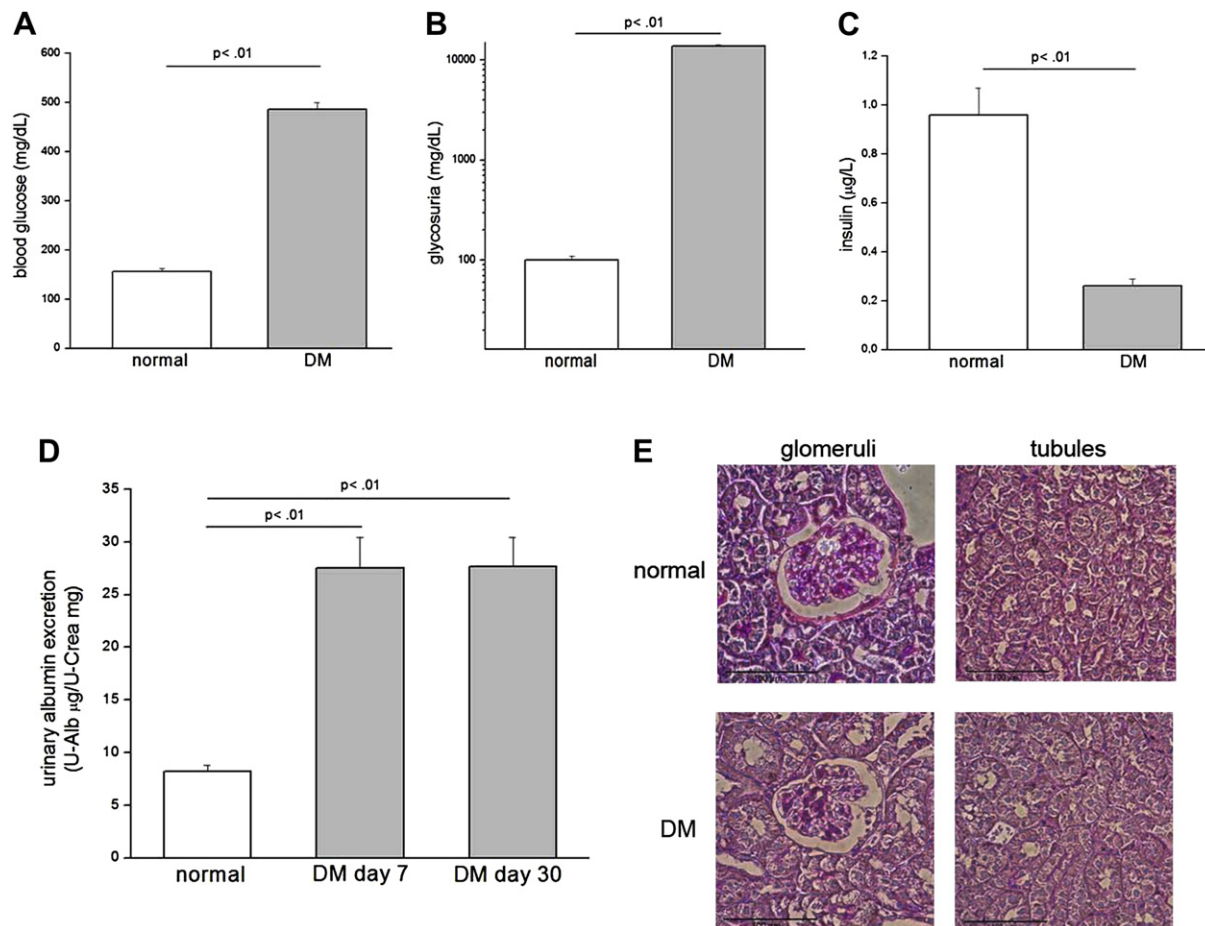


Figure 2. Characterization of diabetes stage in mice that will be treated with MSC. C57BL/6 adult male mice were injected either with 0.1 M citrate buffer (normal) or 200 mg/kg STZ in 0.1 M citrate buffer (DM). Thirty days after STZ injection, blood glucose level was determined in venous blood samples obtained from alert nonfasted animals (A); glycosuria was determined in morning spot urine samples (B); blood insulin level was determined in venous blood samples obtained from alert fasted animals (C); urinary albumin excretion was determined in morning spot urine samples according to albumin to creatinine concentration assessed by the use of commercial kits (D); and renal histology was studied in serial 4- μ m PAS-stained sections, observed under light microscopy and focusing on glomeruli and tubule structures (E). Quantitative data shown correspond to the mean \pm SEM of 10 animals per experimental group. Qualitative data shown are representative of 25 sections per animal, for 4 animals per experimental group. Only significant *P* values are shown.

Pancreas Double-Label Immunohistofluorescence

Deparaffinized pancreatic sections were incubated for 2 hours with chicken antihuman insulin from Chemicon (Temecula, CA) and rabbit antiporcine glucagon from DAKO (Carpinteria, CA). After washing, the sections were incubated for 1 hour with Alexa 594 conjugated antichick IgG and Alexa 488 conjugated antirabbit IgG from Molecular Probes (Eugene, OR). Crossreactivity of secondary antibodies was tested by replacing the target primary antibody with normal serum. Slices were examined under laser scanning confocal microscope and 1- μ m optical sections were analyzed [39].

Donor MSC^{GFP} Detection in Recipient Organs

Seven and 90 days after MSC^{GFP} administration to DM or to normal nondiabetic mice, kidneys, BM, and heart were obtained from sacrificed animals, weighted and washed twice with ice-cold PBS. Organs were chopped and digested with 2 mg/mL collagenase type II (Gibco, Auckland, NZ), 30 min at 37°C. Cell suspension thus obtained was filtered through a 100- μ m strainer and washed twice with ice-cold PBS. High autofluorescence of kidney cells impairs GFP detection [40,41]. Hence, to ensure MSC^{GFP} recognition, isolated cells were resuspended, fixed, permeabilized with BD Cytofix/Cytoperm kit (BD

Biosciences), and resuspended in 1 mL of PBS with 2% fetal bovine serum plus 0.5 μ L of undiluted antibody anti-GFP Alexa Fluor 647 (Molecular Probes). After 24 hours of incubation at 4°C, the cells were washed, filtered through a 30- μ m mesh, and acquired in a CyAn ADP flow cytometer (DakoCytomation) as described for lymphocyte homing studies [42,43]. Data were analyzed with Summit v4.3 software, and criteria used to consider an event as an MSC^{GFP} were FSC and SSC similar to ex vivo expanded MSC and positive fluorescence, both in FL1 (GFP) and FL8 (anti GFP-Alexa Fluor 647) channels. For each organ, acquisition was performed up to the detection of 100 events that fulfilled the criteria of an MSC^{GFP}. In the case of organs where donor MSC were undetectable, a total of 500,000 events were acquired. The frequency of donor MSC was expressed as the number of MSC^{GFP} detected in 1 organ. This technique was validated by ex vivo injecting 1000 MSC^{GFP} to the kidney, BM, and heart. The recovery of MSC^{GFP} was 90% to 99%.

Statistical Analysis

Data are presented as mean \pm SEM. Multiple comparisons between groups were performed using analysis of variance (ANOVA), followed by a Bonferroni multiple comparison test, and values of $P < .05$ were considered statistically significant. All analyses were

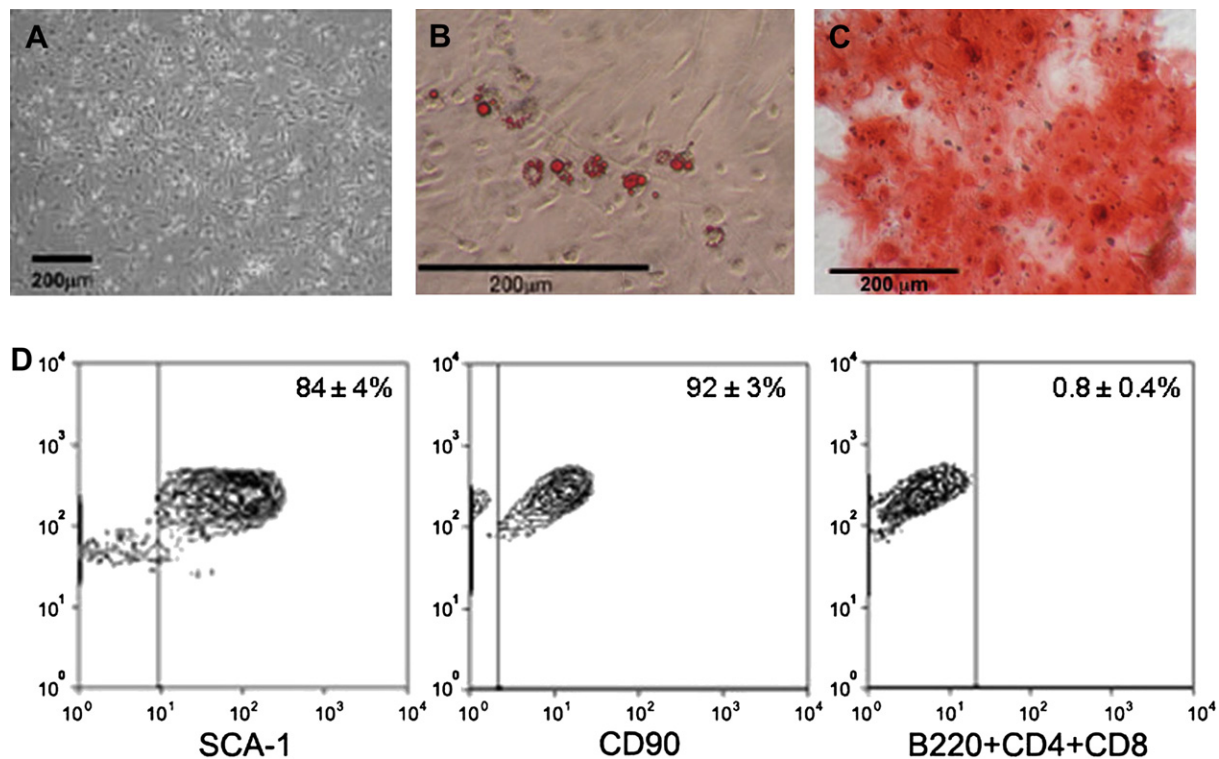


Figure 3. Characterization of bone marrow-derived MSC isolated from C57BL/6 adult male mice. Bone marrow cells were cultured in alpha-MEM containing 10% selected fetal bovine serum into plastic dishes. Plastic adherent cells were ex vivo expanded (A) and differentiated into adipogenic (B) or osteogenic (C) lineages. Cells were also immunophenotyped according to the expression of SCA-1 and CD90, and no-expression of B220, CD4, and CD8 antigens (D). Data shown are representative of cells isolated from 4 different animals.

made using GraphPad Prism 4.0 (GraphPad Software, San Diego, CA).

RESULTS

In the present work, nonimmunologic severe diabetes was induced in C57BL/6 mice by the injection of a single dose of 200 mg/kg STZ, a protocol that causes rapid and massive β -pancreatic cell destruction. Mice thus generated (DM mice) were maintained without insulin treatment to allow for the progression of severe diabetes and the appearance of its complications.

At day 30 post-STZ injection, blood glucose levels of DM mice increased from normal values (156 ± 5 mg/dL) to severe hyperglycemia (482 ± 19 mg/dL) (Figure 2A). Together, in DM mice glycosuria was 130 times higher ($13,000 \pm 600$ versus 100 ± 10 mg/dL) and blood insulin values were 3 times lower than those in normal nondiabetic animals (0.26 ± 0.03 versus 0.96 ± 0.11 μ g/L) (Figure 2B and C).

STZ, when used at high doses, has a modest nephrotoxic effect [44]. Accordingly, 7 days post-STZ injection, a discrete increase in albuminuria was observed (27 ± 3 U-Alb μ g/U-Crea mg) (Figure 2D). However, this level did not change up to 30 days (Figure 2D) and did not associate with any glomerular or tubular histopathologic alterations (Figure 2E). Thus, it was considered as a baseline.

At day 30 post-STZ injection, animals were randomly assigned into 2 groups: untreated DM mice received the vehicle and MSC-treated DM mice received 2 doses (day 30 and 51) of 0.5×10^6 BM-derived

MSC (Figure 1) that have been ex vivo expanded and characterized according to their plastic adherence, mesenchymatic differentiation potential, and immunophenotype (Figure 3). During the study period, 35% (7/20) of untreated DM mice and 25% (5/20) of MSC-treated DM mice died or had to be killed because of severe weight loss and cachexia. These animals were excluded from data analysis.

As seen in Figure 4, untreated DM mice gradually increased albumin excretion rate. Four months after diabetes onset, they reached values 15 times higher than that of age matched normal nondiabetic animals (124 ± 31 versus 8 ± 1 U-Alb μ g/U-Crea mg). In contrast, MSC-treated diabetic mice maintained low levels of albuminuria up to the end of the study period (27 ± 7 U-Alb μ g/U-Crea mg).

When kidney weight to body weight ratio was calculated, a 2-fold increase on it was observed in DM mice compared to normal nondiabetic mice (14 ± 4 mg/g versus 6.4 ± 0.4 mg/g, respectively). No significant change was associated with MSC administration (13 ± 5 mg/g). However, kidney function protection achieved by MSC administration into DM mice correlated with renal structure preservation. By light microscopy, we observed glomerular sclerosis (Figure 5C), mesangial expansion (Figure 5E), marked tubular dilatation (Figure 5D), and proteins cylinders (Figure 5F) in untreated DM mice. However, in MSC-treated DM mice glomeruli appeared normal (Figure 5G) and some tubules showed only minor dilatation (Figure 5H), when compared to that of normal nondiabetic mice (Figure 5A and B). MSC administration was associated with a small percentage of

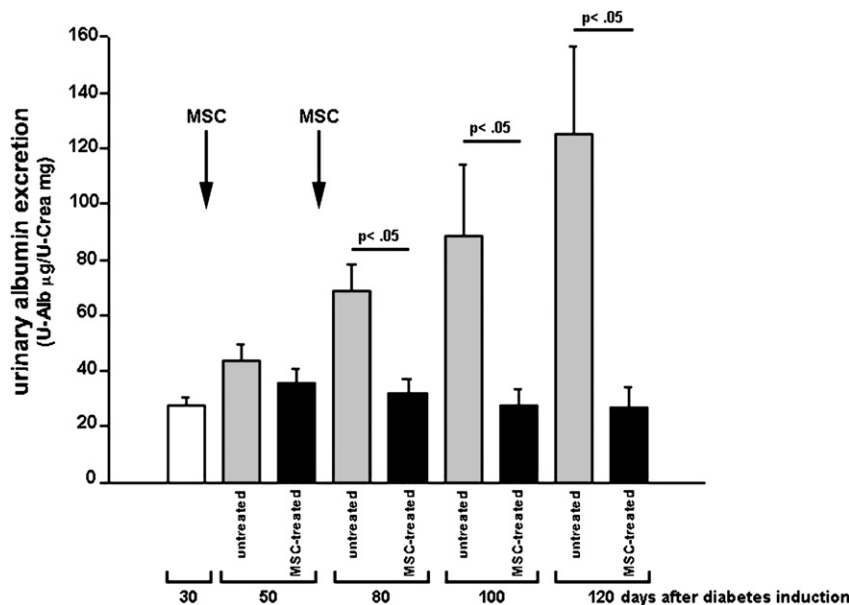


Figure 4. Prevention of renal failure in MSC-treated DM mice: functional data. Thirty and 51 days after STZ injection, mice received 0.2 mL of 5% mice plasma (untreated) or 0.5×10^6 MSC resuspended in 0.2 mL of 5% mice plasma (MSC treated) via the tail vein. At day 30, 50, 80, 100, and 120 post-STZ injection, urinary albumin excretion was determined in morning spot urine samples according to albumin to creatinine concentrations, which were assessed by commercial kits. Data shown correspond to the mean \pm SEM of 8 animals per experimental group. Only significant *P* values are shown.

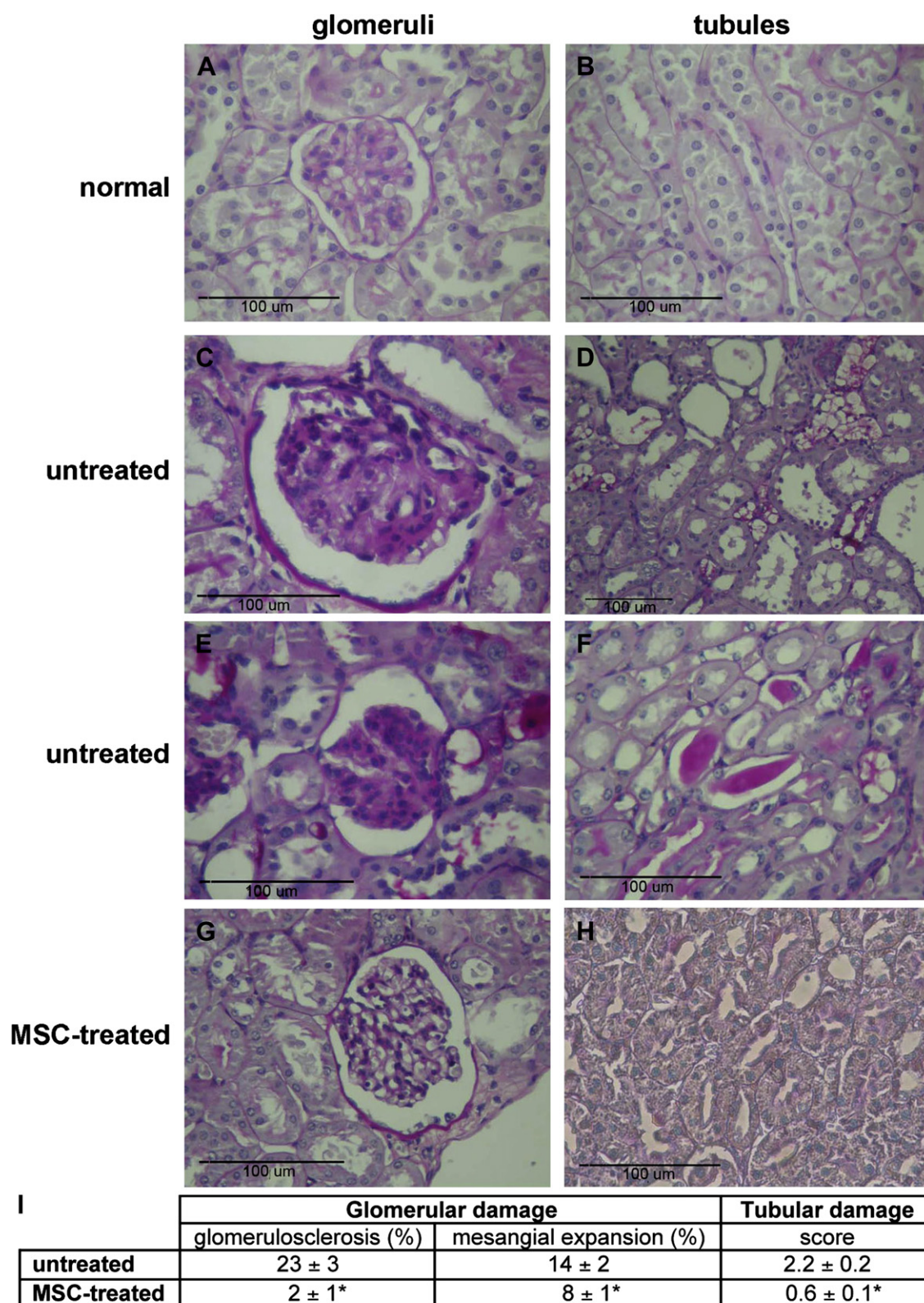


Figure 5. Prevention of renal failure in MSC-treated DM mice: structural data. Thirty and 51 days after STZ injection, mice received 0.2 mL of 5% mice plasma (untreated) or 0.5×10^6 MSC resuspended in 0.2 mL of 5% mice plasma (MSC treated) via the tail vein. One hundred twenty days post-STZ injection, renal histology was studied in serial 4- μ m PAS-stained sections, observed under light microscopy and focusing on glomeruli and tubule structures. Normal nondiabetic animals glomeruli (A) and tubules (B). Untreated DM mice glomerular sclerosis (C), glomerular mesangial expansion (E), tubular dilatation (D), and tubular protein cylinders (F). MSC-treated DM mice glomeruli (G), and tubules (H). Glomerular and tubular damage quantification in untreated and MSC-treated DM mice (I). Data shown are representative of 25 sections per animal and correspond to the mean \pm SEM of 4 animals per experimental group. Only significant P values are shown.

glomeruli with sclerotic changes as well as to less tubular damage (Figure 5I). Electron microscopy analysis of kidneys of untreated DM mice revealed regions of mesangial expansion and podocyte loss in the glomerular structures (Figure 6C) and cytoplasmic vacuoles in tubular cells (Figure 6D). However, kidneys of MSC-treated DM mice (Figure 6E and F) showed glomerular and tubular ultrastructures similar to those of normal nondiabetic animals (Figure 6A and B). Glomerular basement membrane thickening was undetectable in all studied animals.

To find out if renoprotection observed after MSC transplantation into severe nonimmunologically induced diabetic mice was secondary to a concomitant improvement of endocrine pancreas function, glycemia was determined throughout the study period. Five days post-STZ injection, DM mice reached hyperglycemic value (480 ± 13 mg/dL) and continued

with elevated blood glucose levels until the end of the study, independently if they received or not MSC (421 ± 23 versus 457 ± 32 mg/dL) (Figure 7A). Accordingly, untreated and MSC-treated DM mice exhibited very low insulinemia compared to normal nondiabetic animals (0.28 ± 0.02 versus 0.96 ± 0.11 μ g/L) (Figure 7B). At the histologic level, β -pancreatic islets were less abundant in untreated and MSC-treated DM mice than in normal nondiabetic animals (9 ± 1 versus 27 ± 4 islet/section) (Figure 7C). Furthermore, the remnant islets were architecturally altered, showing rare insulin producing cells and a massive expansion of glucagon producing cells (Figure 7D). Thus, in contrast to what we have previously reported in an immunologically induced diabetes model [25], in this nonimmunologically induced diabetes model, MSC administration did not improve diabetes condition.

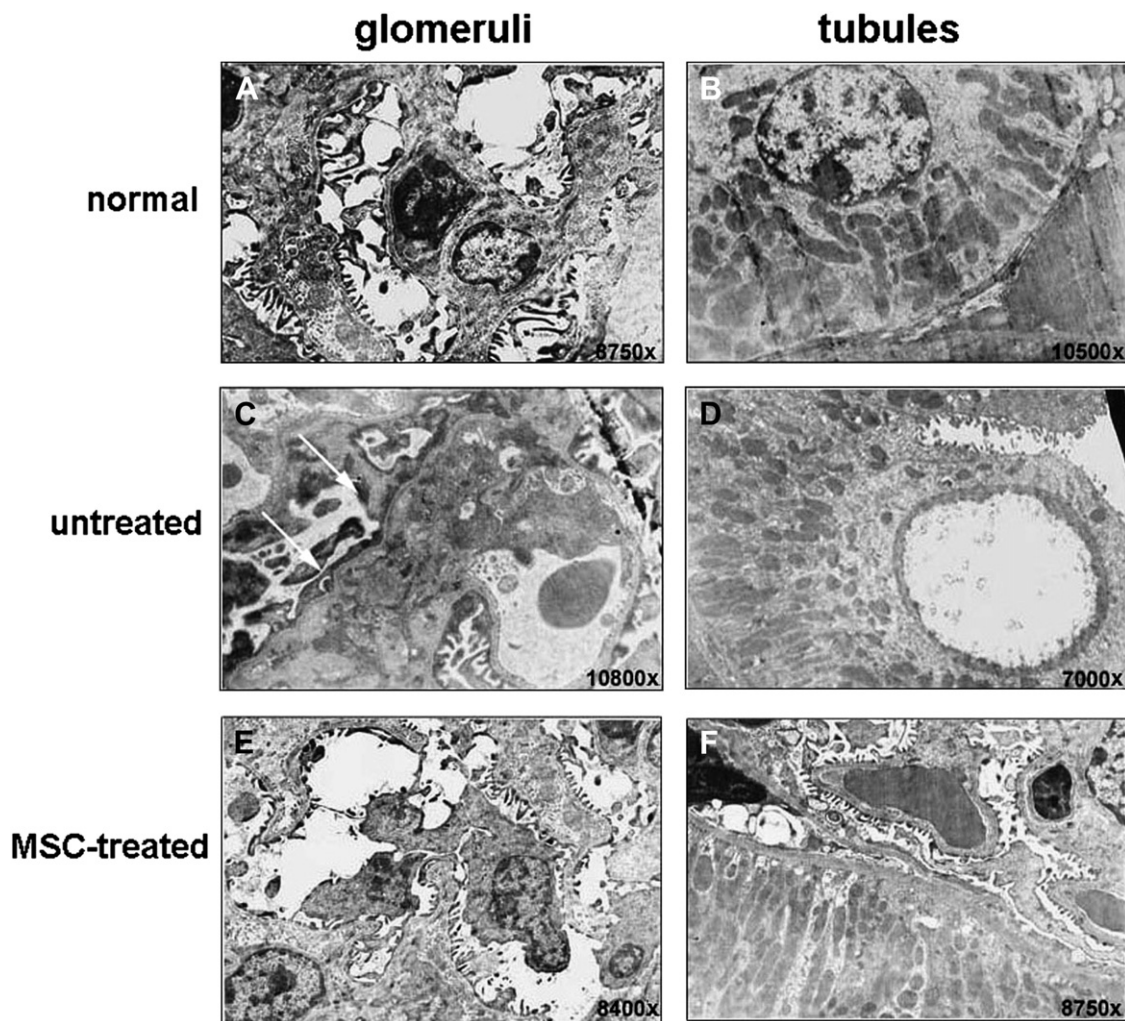


Figure 6. Prevention of renal failure in MSC-treated DM mice: ultrastructural data. Thirty and 51 days after STZ injection, mice received 0.2 mL of 5% mice plasma (untreated) or 0.5×10^6 MSC resuspended in 0.2 mL of 5% mice plasma (MSC treated) via the tail vein. One hundred twenty days post-STZ injection, renal histology was studied in ultrathin sections, observed under electron microscopy and focusing on glomeruli and tubule structures. Normal nondiabetic animals glomeruli (A) and tubules (B). Untreated DM mice glomerular mesangial expansion and podocyte lost (C) and tubular cell with cytoplasmic vacuole (D). MSC-treated DM mice glomeruli (E) and tubules (F). Data shown are representative of 10 sections per animal, for 4 animals per experimental group.

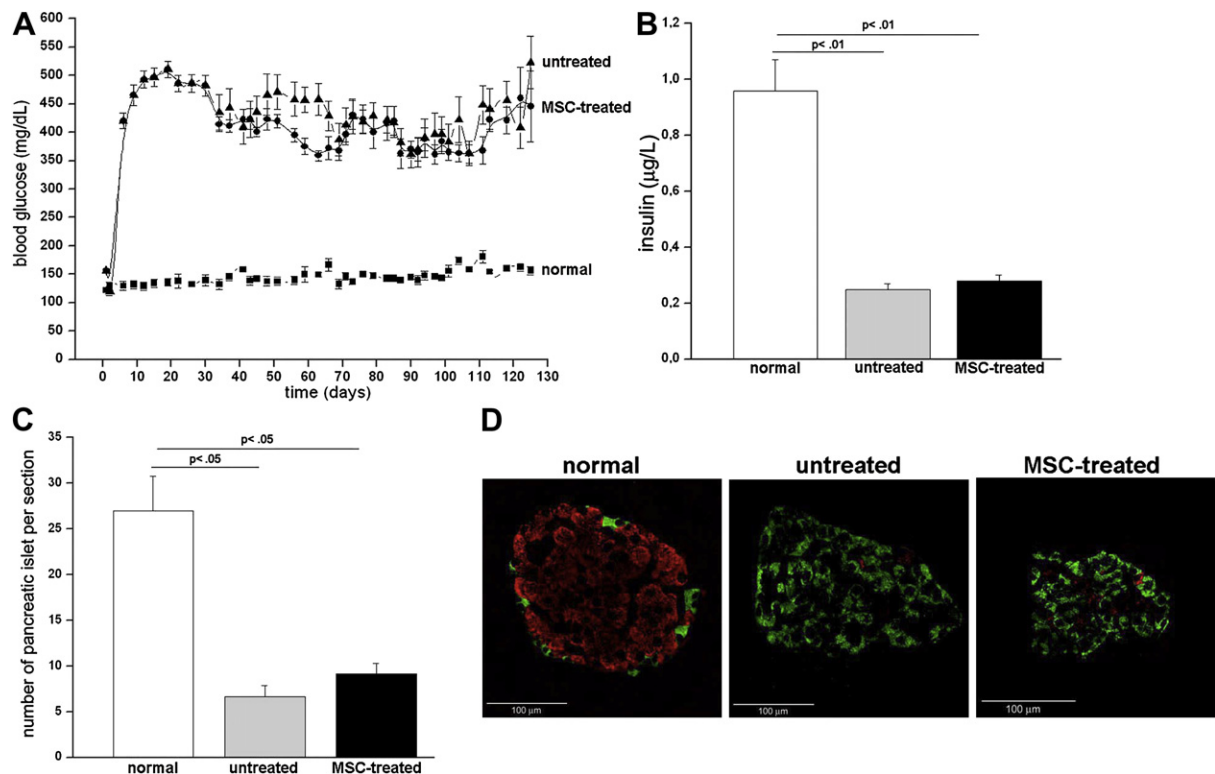


Figure 7. No improvement of endocrine pancreas function in MSC-treated DM mice. Thirty days and 51 days post-STZ injection, mice received 0.2 mL of 5% mice plasma (untreated) or 0.5×10^6 MSC resuspended in 0.2 mL of 5% mice plasma (MSC treated) via the tail vein. Every 3 days, blood glucose level was determined in alert nonfasted animals using the Accu-Chek Go system (A). One hundred twenty days post-STZ injection, blood insulin level was determined in venous blood samples obtained from alert fasted animals (B); β -pancreatic islets were quantified in serial 4- μ m hematoxylin/eosin-stained sections, observed under light microscopy (C); β -pancreatic islets were characterized by immunohistochemistry according to the presence and distribution of insulin- and glucagon-producing cells (red and green, respectively) (D). Quantitative data shown correspond to the mean \pm SEM of 8 animals per experimental group. Qualitative data shown are representative of 25 sections per animal, for 4 animals per experimental group.

Finally, the biodistribution of MSC in severe non-immunologically induced diabetic mice was assessed and compared to normal nondiabetic mice. Donor MSC were found into the kidney and the BM of DM mice 7 days postadministration (Figure 8A). However MSC^{GFP} were undetectable in any of the tested organs obtained from normal nondiabetic mice (Figure 8B). Eventhough there was a significant interanimal variability in the amount of MSC^{GFP} detected in DM mice (Figure 8C), data appear to be reliable because negative organs were always negative (e.g., heart) and relative abundance of donor cells was maintained across organ types for a fixed time (e.g., 90 days after MSC^{GFP} administration into DM mice, the BM is the organ with highest frequency of donor cells in all animal tested).

Thus, a small number of donor cells homed (day 7) and persisted (day 90) both in the kidney and the BM of DM mice (Figure 8C).

DISCUSSION

Hyperglycemia is a major risk factor for DN [7], but other features like glycation end-products and overexpression of different growth factors are also

associated with its pathogenesis [16]. Extracellular matrix accumulation is one of the hallmarks in the development of the disease that leads to the formation of glomerular and interstitial lesions [15]. Recent studies suggest that inflammatory processes and immune cells might be involved in the development and progression of DN [45]. Thus, macrophages, neutrophils, and T lymphocyte migration and activation into the kidney, maintain a chronic inflammatory process that is crucial for parenchyma and vascular injury. Although, the kidney possesses a remarkable regenerative capacity [46], the persistent presence of former noxas results in renal failure in diabetic individuals. Thus, an ideal therapeutic strategy for DN might contribute to kidney regeneration through the replenishment of renal cells and/or managing pathogenic factors. Here, we show that endovenous administration of syngeneic MSC prevents renal failure in diabetic mice eventhough there was no improvement in diabetes condition.

Previously we reported that systemic administration of MSC into immunologically induced type 1 diabetic mice reduced microalbuminuria and preserved normal renal histology [25]. By contrast, untreated type 1 diabetic mice developed the early harbingers of DN (mild microalbuminuria and tubular and glomerular hyalinosis). In that work, renal protection

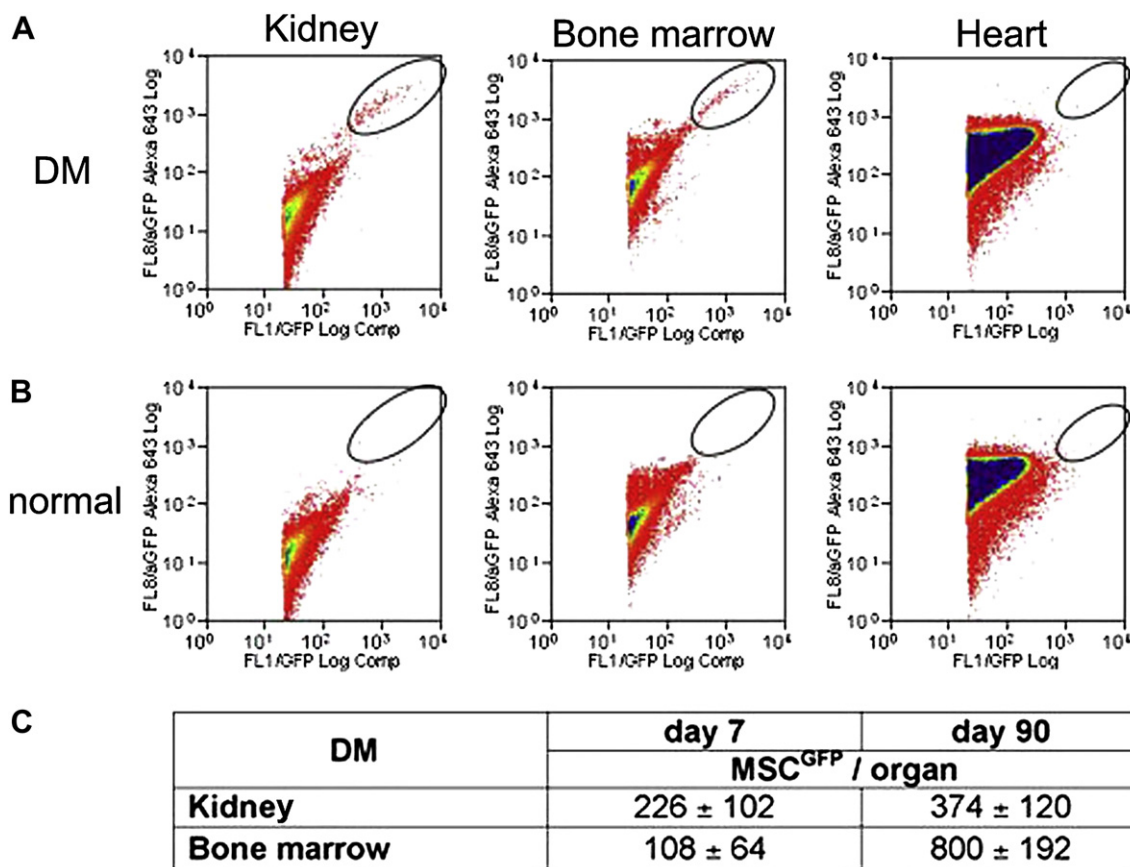


Figure 8. Donor MSC^{GFP} were detected in the kidney and bone marrow of DM mice, but not in normal nondiabetic mice. A half million of MSC^{GFP} resuspended in 0.2 mL of 5% mice plasma were administered via the tail vein to receptors. Seven days later, the presence of donor cells into kidneys, bone marrow, and heart of DM mice (A) or normal nondiabetic mice (B) was assessed by flow cytometry. Events that appear in gate shown were considered as MSC^{GFP}. Plots are representative data for organs obtained from 4 DM mice and 4 normal nondiabetic mice. The absolute numbers of donor cells found in kidney and bone marrow of DM mice, 7 and 90 days after MSC^{GFP} administration were expressed as the mean ± SEM of data obtained for 4 animals per time (C).

was associated with a clear reduction in hyperglycemia, because of the functional recovery of insulin-producing cells and the regeneration of β -pancreatic structures. In contrast, in the nonimmunologically induced diabetes model, MSC administration reverted neither hyperglycemia nor hypoinsulinemia, suggesting that the contribution of transplanted MSC to β -pancreatic cell regeneration depends on the etiology of diabetes; that is, on the mechanism by which β -pancreatic cells have been destroyed. Interestingly, even if hyperglycemia remains high, renal failure did not progress in MSC-treated DM mice, although in untreated DM mice, microalbuminuria gradually increased, and at the end of the study renal histopathologic alterations were evident.

To determine whether renoprotection associated with MSC administration is related to the recruitment of donor cells into the kidneys, we evaluated the biodistribution of MSC^{GFP} once administered in DM mice. One week or 3 months after administration, donor cells were found in the kidney of DM mice (226 ± 102 and 374 ± 120 donor cells/kidney, respectively). MSC^{GFP} were also found in the BM but not

in the heart of DM mice. On the other hand, donor MSC neither home nor persist in any tested organ of normal nondiabetic mice, suggesting that signals produced by damage tissues are required for MSC lodgment into the organs of DM mice [47]. The small number of donor cells detected in the kidneys of diabetic receptor either 7 or 90 days postadministration indicates a discrete renotropism of MSC, and make hard to explain the observed beneficial effect in kidneys of diabetic mice through a differentiation mechanism, as has been described in some acute renal damage models [48,49]. Accordingly, recently it has been shown that the major cell source for kidney regeneration and homeostasis are the intrarenal cells [40,41].

Rare donor cells that persist in the kidney of diabetic animals might have a therapeutic effect because of their ability to produce renotrophic factors or anti-inflammatory cytokines [50-52]. For instance, it is already known that MSC secrete hepatocyte growth factor, vascular endothelial growth factor, and bone morphogenic factors, which promote mitogenic, anti-apoptotic, and morphogenic activities of intrarenal

cells [53-55]. MSC also produce IL-10, which generates a protective microenvironment that might avoid the immunologic destruction of renal cells [53]. On the other hand, MSCs might contribute to the remodeling of the extracellular matrix, and hence, abrogate renal structural damage [56]. Currently, we are studying the relative contribution of those potential mechanisms in renoprotection observed after systemic administration of MSC into DM mice.

Our preclinical results support endovenous administration of MSC as a cell therapy strategy that, without recipient preconditioning, will prevent chronic renal diseases secondary to diabetes even if hyperglycemia condition remains uncorrected.

ACKNOWLEDGMENTS

The authors thank Mrs. Micaela Ricca for assistance with animal care and Mrs. Carolina Larrain for English editing of the manuscript. This work was supported by grants PBCT PSD-34 to P.C. and FONDECYT No. 1051057 to A.Y.

Financial disclosure: The authors have nothing to disclose.

REFERENCES

1. Zimmet P, Alberti KG, Shaw J. Global and societal implications of the diabetes epidemic. *Nature*. 2001;414:782-787.
2. Wild S, Roglic G, Green A, Sicree R, King H. Global prevalence of diabetes: estimates for the year 2000 and projections for 2030. *Diabetes Care*. 2004;27:1047-1053.
3. Remuzzi G, Schieppati A, Ruggerenti P. Clinical practice. Nephropathy in patients with type 2 diabetes. *N Engl J Med*. 2002;346:1145-1151.
4. USRDS. The United States Renal Data System. *Am J Kidney Dis*. 2003;42:1-230.
5. Maisonville P, Agodoa L, Gellert R, et al. Distribution of primary renal diseases leading to end-stage renal failure in the United States, Europe, and Australia/New Zealand: results from an international comparative study. *Am J Kidney Dis*. 2000;35:157-165.
6. Chavers BM, Bilous RW, Ellis EN, Steffes MW, Mauer SM. Glomerular lesions and urinary albumin excretion in type I diabetes without overt proteinuria. *N Engl J Med*. 1989;320:966-970.
7. Cooper ME. Pathogenesis, prevention, and treatment of diabetic nephropathy. *Lancet*. 1998;352:213-219.
8. Schena FP, Gesualdo L. Pathogenetic mechanisms of diabetic nephropathy. *J Am Soc Nephrol*. 2005;16:S30-S33.
9. Wolfe RA, Ashby VB, Milford EL, et al. Comparison of mortality in all patients on dialysis, patients on dialysis awaiting transplantation, and recipients of a first cadaveric transplant. *N Engl J Med*. 1999;341:1725-1730.
10. Koya D, Hayashi K, Kitada M, Kashiwagi A, Kikkawa R, Haneda M. Effects of antioxidants in diabetes-induced oxidative stress in the glomeruli of diabetic rats. *J Am Soc Nephrol*. 2003;14:S250-S253.
11. Kim YH, Goyal M, Kurnit D, et al. Podocyte depletion and glomerulosclerosis have a direct relationship in the PAN-treated rat. *Kidney Int*. 2001;60:957-968.
12. Siu B, Saha J, Smoyer WE, Sullivan KA, Brosius FC. Reduction in podocyte density as a pathologic feature in early diabetic nephropathy in rodents: prevention by lipoic acid treatment. *BMC Nephrol*. 2006;7:6.
13. Chow FY, Nikolic-Paterson DJ, Ozols E, Atkins RC, Rollin BJ, Tesch GH. Monocyte chemoattractant protein-1 promotes the development of diabetic renal injury in streptozotocin-treated mice. *Kidney Int*. 2006;69:73-80.
14. Furuta T, Saito T, Ootaka T, et al. The role of macrophages in diabetic glomerulosclerosis. *Am J Kidney Dis*. 1993;21:480-485.
15. Chow FY, Nikolic-Paterson DJ, Atkins RC, Tesch GH. Macrophages in streptozotocin-induced diabetic nephropathy: potential role in renal fibrosis. *Nephrol Dial Transplant*. 2004;19:2987-2996.
16. Chow FY, Nikolic-Paterson DJ, Ozols E, Atkins RC, Tesch GH. Intercellular adhesion molecule-1 deficiency is protective against nephropathy in type 2 diabetic db/db mice. *J Am Soc Nephrol*. 2005;16:1711-1722.
17. Rodby RA, Rohde R, Evans J, Bain RP, Mulcahy WS, Lewis EJ. The study of the effect of intensity of blood pressure management on the progression of type 1 diabetic nephropathy: study design and baseline patient characteristics. Collaborative Study Group. *J Am Soc Nephrol*. 1995;5:1775-1781.
18. Dressler RL. Antihypertensive agents for prevention of diabetic nephropathy. *Am Fam Physician*. 2006;74:77-79.
19. Yamagishi S, Fukami K, Ueda S, Okuda S. Molecular mechanisms of diabetic nephropathy and its therapeutic intervention. *Curr Drug Targets*. 2007;8:952-959.
20. Caplan AI. The mesengenic process. *Clin Plast Surg*. 1994;21:429-435.
21. Herrera MB, Bussolati B, Bruno S, Fonsato V, Romanazzi GM, Camussi G. Mesenchymal stem cells contribute to the renal repair of acute tubular epithelial injury. *Int J Mol Med*. 2004;14:1035-1041.
22. Fang TC, Alison MR, Cook HT, Jeffery R, Wright NA, Poulosom R. Proliferation of bone marrow-derived cells contributes to regeneration after folic acid-induced acute tubular injury. *J Am Soc Nephrol*. 2005;16:1723-1732.
23. Wong CY, Cheong SK, Mok PL, Leong CF. Differentiation of human mesenchymal stem cells into mesangial cells in post-glomerular injury murine model. *Pathology*. 2008;40:52-57.
24. Sugimoto H, Mundel TM, Sund M, Xie L, Cosgrove D, Kalluri R. Bone-marrow-derived stem cells repair basement membrane collagen defects and reverse genetic kidney disease. *Proc Natl Acad Sci USA*. 2006;103:7321-7326.
25. Ezquer FE, Ezquer ME, Parrau DB, Carpio D, Yanez AJ, Conget PA. Systemic administration of multipotent mesenchymal stromal cells reverts hyperglycemia and prevents nephropathy in type 1 diabetic mice. *Biol Blood Marrow Transplant*. 2008;14:631-640.
26. Lee RH, Seo MJ, Reger RL, et al. Multipotent stromal cells from human marrow home to and promote repair of pancreatic islets and renal glomeruli in diabetic NOD/scid mice. *Proc Natl Acad Sci USA*. 2006;103:17438-17443.
27. Katoh M, Ohmachi Y, Kurosawa Y, Yoneda H, Tanaka N, Narita H. Effects of imidapril and captopril on streptozotocin-induced diabetic nephropathy in mice. *Eur J Pharmacol*. 2000;398:381-387.
28. Grover JK, Vats V, Rathi SS, Dawar R. Traditional Indian anti-diabetic plants attenuate progression of renal damage in streptozotocin induced diabetic mice. *J Ethnopharmacol*. 2001;76:233-238.
29. Thirone AC, Scarlett JA, Gasparetti AL, et al. Modulation of growth hormone signal transduction in kidneys of streptozotocin-induced diabetic animals: effect of a growth hormone receptor antagonist. *Diabetes*. 2002;51:2270-2281.
30. Okada S, Shikata K, Matsuda M, et al. Intercellular adhesion molecule-1-deficient mice are resistant against renal injury after induction of diabetes. *Diabetes*. 2003;52:2586-2593.
31. Gabra BH, Sirois P. Beneficial effect of chronic treatment with the selective bradykinin B1 receptor antagonists, R-715 and R-954, in attenuating streptozotocin-diabetic thermal hyperalgesia in mice. *Peptides*. 2003;24:1131-1139.

32. Dogrul A, Gul H, Yildiz O, Bilgin F, Guzeldemir ME. Cannabinoids blocks tactile allodynia in diabetic mice without attenuation of its antinociceptive effect. *Neurosci Lett*. 2004;368:82-86.
33. Conget PA, Minguell JJ. Phenotypical and functional properties of human bone marrow mesenchymal progenitor cells. *J Cell Physiol*. 1999;18:67-73.
34. Dominici M, Le Blanc K, Mueller I, et al. Minimal criteria for defining multipotent mesenchymal stromal cells. The International Society for Cellular Therapy position statement. *Cytotherapy*. 2006;8:315-317.
35. Kinnaird T, Stabile E, Burnett MS, et al. Marrow-derived stromal cells express genes encoding a broad spectrum of arteriogenic cytokines and promote in vitro and in vivo arteriogenesis through paracrine mechanisms. *Circ Res*. 2004;94:678-685.
36. Wakasugi S, Maeda S, Shimada K, et al. Structural comparisons between mouse and human prealbumin. *J Biochem*. 1985;98:1707-1714.
37. Benigni A, Zoja C, Zatelli C, et al. Vasoepitaxial inhibitor restores the balance of vasoactive hormones in progressive nephropathy. *Kidney Int*. 2004;66:1959-1965.
38. Hayakawa M, Shibata M. The in vitro and in vivo inhibition of protein glycosylation and diabetic vascular basement membrane thickening by pyridoxal-5'-phosphate. *J Nutr Sci Vitaminol (Tokyo)*. 1991;37:149-159.
39. Yanez AJ, Bertinat R, Spichiger C, et al. Novel expression of liver FBPase in Langerhans islets of human and rat pancreas. *J Cell Physiol*. 2005;205:19-24.
40. Duffield JS, Park KM, Hsiao LL, et al. Restoration of tubular epithelial cells during repair of the postischemic kidney occurs independently of bone marrow-derived stem cells. *J Clin Invest*. 2005;115:1743-1755.
41. Lin F, Moran A, Igarashi P. Intrarenal cells, not bone marrow-derived cells, are the major source for regeneration in postischemic kidney. *J Clin Invest*. 2005;115:1756-1764.
42. Li R, Perez N, Karumuthil-Melethil S, Vasu C. Bone marrow is a preferential homing site for autoreactive T-cells in type 1 diabetes. *Diabetes*. 2007;56:2251-2259.
43. Allers K, Kunkel D, Moos V, et al. Migration patterns of non-specifically activated versus nonactivated nonhuman primate T lymphocytes: preferential homing of activated autologous CD8 + T cells in the rectal mucosa. *J Immunother*. 2008;31:334-344.
44. Tay YC, Wang Y, Kairaitis L, Rangan GK, Zhang C, Harris DC. Can murine diabetic nephropathy be separated from superimposed acute renal failure? *Kidney Int*. 2005;68:391-398.
45. Galkina E, Ley K. Leukocyte recruitment and vascular injury in diabetic nephropathy. *J Am Soc Nephrol*. 2006;17:368-377.
46. Liu KD, Brakeman PR. Renal repair and recovery. *Crit Care Med*. 2008;36:S187-S192.
47. Uccelli A, Moretta L, Pistoia V. Mesenchymal stem cells in health and disease. *Nat Rev Immunol*. 2008;8:726-736.
48. Imasawa T, Utsunomiya Y, Kawamura T, et al. The potential of bone marrow-derived cells to differentiate to glomerular mesangial cells. *J Am Soc Nephrol*. 2001;12:1401-1409.
49. Morigi M, Imberti B, Zoja C, et al. Mesenchymal stem cells are renotropic, helping to repair the kidney and improve function in acute renal failure. *J Am Soc Nephrol*. 2004;15:1794-1804.
50. Semedo P, Palasio CG, Oliveira CD, et al. Early modulation of inflammation by mesenchymal stem cell after acute kidney injury. *Int Immunopharmacol*. 2009 [Epub ahead of print].
51. Le Blanc K. Mesenchymal stromal cells: tissue repair and immune modulation. *Cytotherapy*. 2006;8:559-561.
52. McTaggart SJ, Atkinson K. Mesenchymal stem cells: immunobiology and therapeutic potential in kidney disease. *Nephrolgy*. 2007;12:44-52.
53. Togel F, Hu Z, Weiss K, Isaac J, Lange C, Westenfelder C. Administered mesenchymal stem cells protect against ischemic acute renal failure through differentiation-independent mechanisms. *Am J Physiol Renal Physiol*. 2005;289:F31-F42.
54. Togel F, Weiss K, Yang Y, Hu Z, Zhang P, Westenfelder C. Vasculotropic, paracrine actions of infused mesenchymal stem cells are important to the recovery from acute kidney injury. *Am J Physiol Renal Physiol*. 2007;292:F1626-F1635.
55. Semedo P, Wang PM, Andreucci TH, et al. Mesenchymal stem cells ameliorate tissue damages triggered by renal ischemia and reperfusion injury. *Transplant Proc*. 2007;39:421-423.
56. Higashiyama R, Inagaki Y, Hong YY, et al. Bone marrow-derived cells express matrix metalloproteinases and contribute to regression of liver fibrosis in mice. *Hepatology*. 2007;45:213-222.